Molecules and Cells

Abrogation of the Circadian Nuclear Receptor REV-ERBα Exacerbates 6-Hydroxydopamine-Induced Dopaminergic Neurodegeneration

Jeongah Kim[1,2], Sangwon Jang[1], Mijung Choi[1], Sooyoung Chung[3], Youngshik Choe[4], Han Kyoung Choe[1,4], Gi Hoon Son[5], Kunsoo Rhee[2], and Kyungjin Kim[1,4,*]

[1]Department of Brain and Cognitive Sciences, Daegu Gyeongbuk Institute of Science and Technology (DGIST), Daegu 42988, Korea, [2]Department of Biological Sciences, College of Natural Sciences, Seoul National University, Seoul 08826, Korea, [3]Department of Brain and Cognitive Sciences, Scranton College, Ewha Womans University, Seoul 03760, Korea, [4]Korea Brain Research Institute (KBRI), Daegu 41068, Korea, [5]Department of Biomedical Sciences, College of Medicine, Korea University, Seoul 02841, Korea
*Correspondence: kyungjin@dgist.ac.kr
http://dx.doi.org/10.14348/molcells.2018.0201
www.molcells.org

Parkinson's disease (PD) is a neurodegenerative disease characterized by progressive degeneration of dopaminergic (DAergic) neurons, particularly in the substantia nigra (SN). Although circadian dysfunction has been suggested as one of the pathophysiological risk factors for PD, the exact molecular link between the circadian clock and PD remains largely unclear. We have recently demonstrated that REV-ERBα, a circadian nuclear receptor, serves as a key molecular link between the circadian and DAergic systems. It competitively cooperates with NURR1, another nuclear receptor required for the optimal development and function of DA neurons, to control DAergic gene transcription. Considering our previous findings, we hypothesize that REV-ERBα may have a role in the onset and/or progression of PD. In the present study, we therefore aimed to elucidate whether genetic abrogation of REV-ERBα affects PD-related phenotypes in a mouse model of PD produced by a unilateral injection of 6-hydroxydopamine (6-OHDA) into the dorsal striatum. REV-ERBα deficiency significantly exacerbated 6-OHDA-induced motor deficits as well as DAergic neuronal loss in the vertebral midbrain including the SN and the ventral tegmental area. The exacerbated DAergic degeneration likely involves neuroinflammation-mediated neurotoxicity. The *Rev-erbα* knockout mice showed prolonged microglial activation in the SN along with the overproduction of interleukin 1β, a pro-inflammatory cytokine, in response to 6-OHDA. In conclusion, the present study demonstrates for the first time that genetic abrogation of REV-ERBα can increase vulnerability of DAergic neurons to neurotoxic insults, such as 6-OHDA, thereby implying that its normal function may be beneficial for maintaining DAergic neuron populations during PD progression.

Keywords: 6-hydroxydoapmine, neurodegeneration, circadian clock, Parkinson's disease, REV-ERBα

INTRODUCTION

Parkinson's disease (PD) is a neurodegenerative disease that is characterized by progressive degeneration of dopaminergic (DAergic) neurons in the substantia nigra pars compacta (SNpc), leading to severe impairment of motor and non-motor functions (Dauer and Przedborski, 2003). Although the pathogenesis of PD is still not completely understood,

Received 9 May, 2018; revised 17 June, 2018; accepted 18 June, 2018; published online 30 July, 2018

eISSN: 0219-1032

sporadic pathogenic processes appear to be the major causes of PD. Genetic and environmental risk factors may determine how susceptible an individual is to these sporadic pathogenic processes (Warner and Schapira, 2003).

Circadian dysfunction has been proposed as one such risk factor for a variety of human diseases, including neurodegenerative diseases (Bechtold et al., 2010; Kondratova and Kondratov, 2012). It is well established that patients suffering from PD frequently experience sleep disturbances and excessive daytime sleepiness (Comella, 2006), key factors which contribute to a lower quality of life and manifest before the PD diagnosis (Abbott et al., 2005). Furthermore, mice with a disrupted circadian rhythm exhibit an increased susceptibility to 1-methyl-4-phenyl-1,2,3,6-tetrahydropyridine (MPTP)-induced motor symptoms, DAergic neuronal loss, and neuroinflammation (Lauretti et al., 2017), strongly supporting the concept that circadian disruption may be a risk factor for PD. Although a recent clinical study has proposed that PD is associated with genetic variations found in several core clock genes, such as *BMAL1 (ARNTL)*, *PER1*, and *REV-ERBα* (Gu et al., 2015), the exact molecular link between circadian clock gene function and the onset and progression of PD, remains largely unclear.

REV-ERBα, a circadian nuclear receptor encoded by the gene *NR1D1*, plays an important role in the regulation of various physiological processes, such as circadian rhythm, metabolism, inflammation, and neurotransmission (Everett and Lazar, 2014). In the feedback loop of the mammalian circadian clock, REV-ERBα was initially found to repress *BMAL1* transcription through competition with transcriptional activators (RORα/β/γ) (Guillaumond et al., 2005; Preitner et al., 2002). Notably, REV-ERBα is enriched in midbrain DA neurons and serves as a key molecular link between the circadian and DAergic systems by controlling both DA biosynthesis and transmission (Chung et al., 2014). Crosstalk between REV-ERBα and NURR1, a neuron-enriched nuclear receptor crucial for the development and function of DAergic neurons, contributes to the circadian properties of the midbrain DA system (Chung et al., 2014). It is therefore plausible that REV-ERBα may play a role in the onset and/or progression of PD. To test this idea, the present study examined whether the genetic abrogation of REV-ERBα in mice influences DA neuron vulnerability to striatal injection of 6-hydroxydopamine (6-OHDA), a widely used model of PD in murines.

MATERIALS AND METHODS

Animals and surgery

Rev-erbα mutant mice were provided by Dr. U. Schibler (University of Geneva) (Preitner et al., 2002). Male C57BL/6J wild type (WT) and *Rev-erbα* knockout (RKO) mice aged 10-16 weeks old were used for experiments. The mice were housed using a 12: 12 h light-dark cycle at a constant temperature (22-23℃). All procedures were approved by the Animal Care and Use Committee of DGIST. To induce the PD-like state, the mice were anesthetized with pentobarbital sodium (50 mg/kg), placed in a stereotaxic device (Stoelting, USA), and injected with 6-hydroxydoapmine (6-OHDA). The 6-OHDA (15 μg in 1.0 μl of 0.9% saline containing 0.02% ascorbate) or vehicle (1.0 μl of 0.9% saline containing 0.02% ascorbate) was injected into the left striatum (relative to the bregma: anterior, +0.6 mm; medial, -2.0 mm; dorsal, -3.5 mm) using a 26-gauge microsyringe at a rate of 0.5 μl/min. After a 15-minute period, the needle was slowly withdrawn.

Behavior tests

Behavioral deficits were examined 3 days, 1 week, and 2 weeks after 6-OHDA infusion. Locomotor asymmetry was measured by forelimb use asymmetry at landing during the cylinder test (Kim et al., 2011). Mice were placed individually in a glass cylinder (diameter: 11 cm, height: 30 cm) for 5 min and the number of forepaw landing contacts was counted. Forelimb preference was scored as [R / (L + R)] × 100, where L is the number of left and R is the number of right forepaw contacts. Motor coordination was also evaluated by measuring the time spent on an accelerating rotarod (B.S. Technolab Inc., Korea) (Monville et al., 2006). Before the test, mice were trained for 5 min on the rotarod at 4 rpm and then allowed to rest for ≥ 60 min. Mice were tested in 3 trials with intervals of ≥ 30 min. During each trial, the rod accelerated from 4 to 40 rpm over a 5-min period and the amount of time it took the mouse to fall was recorded. The falling times from the 3 trials were averaged and analyzed.

Immunohistochemistry

Mice were sacrificed 3 days, 1 week, and 2 weeks after injection. Immunohistochemistry was performed as previously described (Chung et al., 2014) with several modifications. Brain sections containing the SNpc and the ventral tegmental area (VTA) were mounted before antigen retrieval was performed in sodium citrate buffer (100℃ for 10 min). The sections were then incubated with antibodies to tyrosine hydroxylase (TH; 1:1000, Abcam, UK), ionized calcium-binding adapter molecule 1 (IBA1; 1:1000, Wako Ltd., Japan), and glial fibrillary acidic protein (GFAP; 1:150, Cell Signaling, USA) overnight at 4℃. After several washes, the samples were incubated in biotinylated secondary antibodies for 1 h and visualized using an avidin-biotin-peroxidase complex kit (Vectastain ABC; Vector Laboratories, USA) and 3-3'-diaminobenzidine reactions. The TH stained sections were examined using an Eclipse 90i microscope (Nikon, Japan), while the IBA1 and GFAP stained sections were evaluated using an Axio Scan Z1 microscope (Carl Zeiss, Germany).

Quantification of TH-positive neurons, microglia, and astrocytes

The number of TH-positive neurons were assessed using the optical dissector method of stereological analysis. Using Stereo Investigator software (MicroBrightField, USA), a fractionator probe was established for each section and 6 sections covering the SNpc and VTA were examined. The border separating the SNpc and VTA was delineated at a lower magnification (Fig. 2A). The number of TH-positive neurons in each counting frame was determined by focusing on the section using a 40x objective lens; the total number in the SNpc and VTA was calculated using the Stereo Investigator

software. Microglia (IBA1-positive cells) and astrocytes (GFAP-positive cells) were counted as the number of stained cells per image (305.73 μm × 305.73 μm) using ImageJ (National Institutes of Health, Bethesda, Maryland, USA). For each glial marker, 4 images were randomly chosen from ipsilateral and contralateral sides of the substantia nigra (SN) from each animal. As each group contained 3-4 animals, 12-16 images were analyzed for each group.

Western blot analysis

Ipsilateral and contralateral VMB tissues were prepared from mice sacrificed at 3 days, 1 and 2 weeks, respectively, after injection. Western blot analysis was performed as previously described (Chung et al., 2014) with modification. Protein samples were resolved on sodium dodecyl sulfate (SDS)-polyacrylamide gels and transferred to PDF membranes (Merck Millipore, France) in a Bio-Rad Trans-Blot electrophoresis apparatus using Towbin's buffer (25 mM Tris [pH 8.3], 192 mM glycine, and 20% methanol). Blots were blocked in Tris-buffered saline (TBS; 10 mM Tris [pH 7.6], 150 mM NaCl, and 2 mM $MgCl_2$) containing 0.3% Tween-20 and 5% bovine serum albumin (BSA) and were incubated with anti-TH (1:500, Sigma-Aldrich, USA) antibodies at room temperature for 1 h. Blots were then washed with TBS containing 0.3% Tween-20. Antibody binding was subsequently detected by incubation with secondary antibodies linked to horseradish peroxidase (Jackson ImmunoResearch Laboratories, USA) at room temperature for 1 h. Blots were washed several times, and immunoreactive bands were visualized by using ChemiDoc XRS system (Bio-Rad, USA) after application of enhanced chemiluminescent (ECL) reagents (Thermo Fisher Scientific, USA).

RNA isolation and reverse transcription-polymerase chain reaction

Ipsilateral and contralateral ventral midbrain (VMB) tissue was prepared from mice sacrificed 1-week post-injection. Isolation of RNA and real-time reverse-transcription PCR were performed as previously described (Chung et al., 2014) with modifications. The primer sequences were: interleukin 1 beta (IL-1β) forward: 5'-GCC CAT CCT CTG TGA CTC AT-3'; IL-1β reverse: 5'-AGG CCA CAG GTA TTT TGT CT-3'; tumor necrosis factor alpha (TNFα) forward: 5'-TCA GCC GAT TTG CTA TCT CA-3'; TNFα reverse: 5'-CGG ACT CCG CAA AGT CTA AG-3'; interleukin 6 (IL-6) forward: 5'-AGT TGC CTT CTT GGG ACT GA-3'; IL-6 reverse: 5'-CAG AAT TGC CAT TGC ACA AC-3'; TATA-box binding protein (TBP) forward: 5'-GGG AGA ATC ATG GAC CAG AA-3'; and TBP reverse: 5'-CCG TAA GGC ATC ATT GGA CT-3'.

Enzyme-linked immunosorbent assay (ELISA)

Ipsilateral and contralateral VMB tissue was prepared from mice sacrificed 3 days, 1 week, and 2 weeks after injection. The tissue was sonicated in a radioimmunoprecipitation assay (RIPA) buffer containing a protease and phosphatase inhibitor cocktail (Thermo Fisher Scientific, USA). Homogenates were centrifuged at 12,000 *g* at 4℃ for 15 min and protein concentrations were determined using the bicinchoninic acid (BCA) protein assay kit (Pierce, USA). The level of IL-1β was quantified with a mouse-specific ELISA kit (R&D systems, USA); the IL-1β content in the VMB tissue was measured as pg/mg protein.

Statistical analysis

All data is reported as mean ± standard error. For RT-PCR, each data set was first screened for outliers using the ROUT method with a Q value of 5.0%. Inter-group differences were evaluated using a two-way analysis of variance (ANOVA) followed by Tukey's post-hoc test. All analyses were performed using GraphPad Prism (version 7.0; GraphPad Software, USA). Statistical significance was set at a p-value of < 0.05.

RESULTS

REV-ERBα deficiency exacerbates motor function impairment

To induce PD, 6-OHDA was unilaterally injected into the dorsal striatum in WT and RKO mice. The degree of motor deficits in the mice was examined 3 days, 1 week, and 2 weeks after 6-OHDA injection using the cylinder and rotarod tests. In the cylinder test, vehicle (VEH)-injected WT and RKO mice used their contralateral forelimbs in approximately 50% of the landing trials, demonstrating symmetrical basal motor function before 6-OHDA administration (Fig. 1A). Three days following 6-OHDA injection, both WT and RKO mice showed significant motor asymmetry; however, there was no significant difference between WT and RKO mice (Fig. 1A). Importantly, 1- and 2-weeks after 6-OHDA injection, motor asymmetry was significantly more severe in RKO mice than in WT animals (Fig. 1A). According to time after 6-OHDA injection, RKO mice exhibited more severe motor asymmetry compared to WT mice (Fig. 1A; $F_{(2,56)} = 6.331$, $p < 0.01$ for time, and $F_{(3,56)} = 181.500$, $p < 0.001$ among groups). There was also significant interaction between time and group ($F_{(6,56)} = 2.433$, $p < 0.05$). Latency to fall on the rotarod test tended to be shorter for VEH-injected RKO than WT mice, but the difference was not statistically significant (Fig. 1B). This is consistent with a previous study which showed that REV-ERBα deficiency impairs exercise capacity (Woldt et al., 2013). Administration of 6-OHDA led to motor deficits in both WT and RKO mice. Interestingly, RKO mice were more susceptible to 6-OHDA-induced motor deficits 1- and 2-weeks after 6-OHDA injection, as measured by the rotarod test (Fig. 1B; $F_{(2,56)} = 0.423$, $p = 0.657$ for time, $F_{(3,56)} = 55.420$, $p < 0.001$ among group, and $F_{(6,56)} = 0.288$, $p = 0.941$ for interaction). These data suggest that REV-ERBα deficiency exacerbates the progression of motor symptoms in a PD model induced by striatal 6-OHDA injection.

6-OHDA induces greater and accelerated DAergic neuronal loss in the SNpc and the VTA in RKO mice

DAergic cell death underlies the PD-like symptoms in the striatal 6-OHDA injection model, with a propagation of retrograde toxicity from the DAergic axon in the striatum to the soma in the VMB, especially in the SNpc (Dauer and Przedborski, 2003; Sauer and Oertel, 1994). Thus, we examined changes in the number of SNpc TH-positive DA neurons

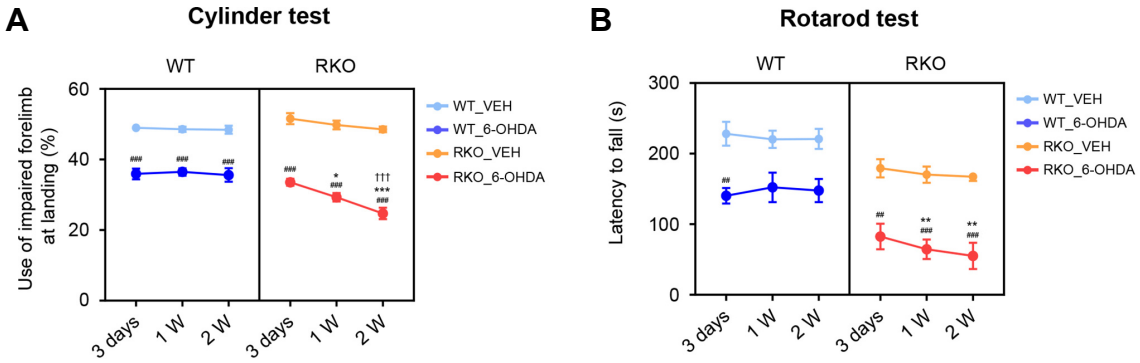

Fig. 1. REV-ERBα deficiency exacerbates motor impairment induced by 6-hydroxydoapmine (6-OHDA). (A) Cylinder tests were performed 3 days, 1 week, and 2 weeks after vehicle (VEH) or 6-OHDA injection in wild type (WT) and *Rev-erbα* knockout (RKO) mice. Data are presented as mean ± standard error. N = 5-7 per group. Two-way analysis of variance was followed by Tukey's post-hoc test; ###p < 0.001 versus VEH-injected group; *p < 0.05, ***p < 0.001 versus WT mice; †††p < 0.001 versus 3 days post-lesion. (B) Rotarod tests were performed 3 days, 1 week, and 2 weeks after the VEH or 6-OHDA injection in WT and RKO mice. Data are presented as mean ± standard error. N = 5-7 per group. Two-way analysis of variance was followed by Tukey's post-hoc test; ##p < 0.01, ###p < 0.001 versus VEH-injected group; **p < 0.01 versus WT mice.

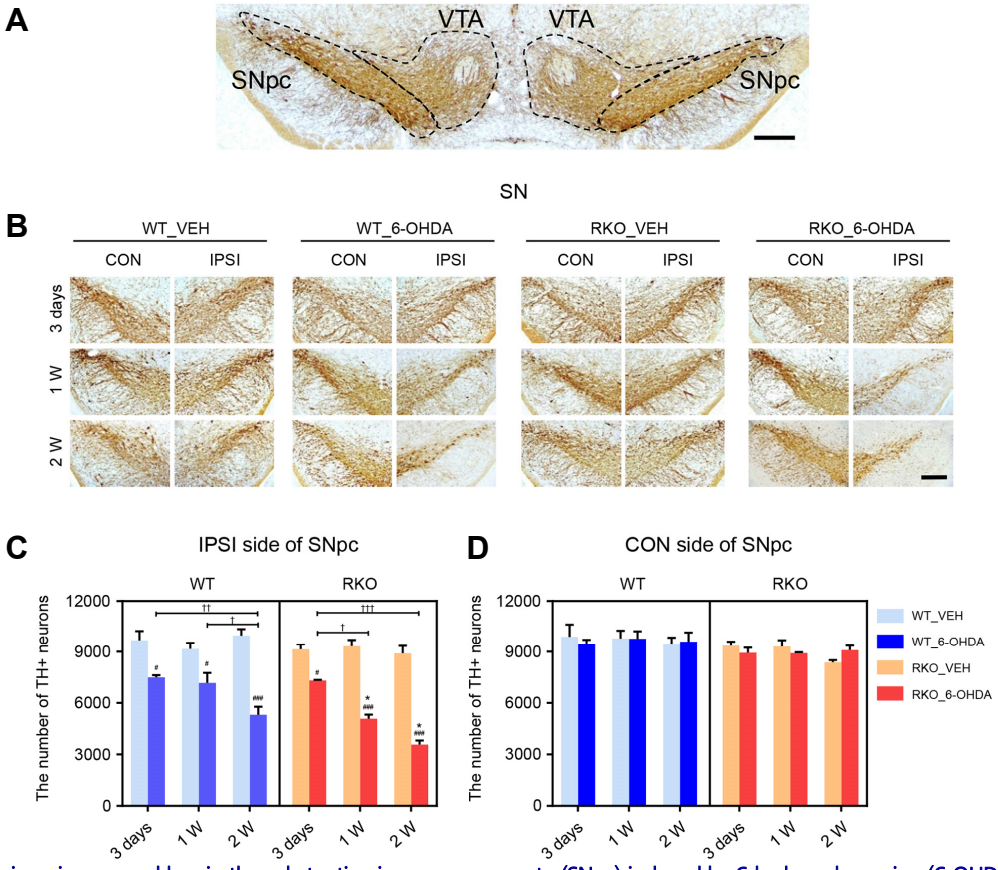

Fig. 2. Dopaminergic neuronal loss in the substantia nigra pars compacta (SNpc) induced by 6-hydroxydoapmine (6-OHDA) is accelerated and intensified in *Rev-erbα* knockout (RKO) mice. (A) Photomicrograph showing the border separating SNpc and ventral tegmental area (VTA) of tissue sections immunostained for tyrosine hydroxylase (TH). Scale bar = 200 μm. (B) Three days, 1 week, and 2 weeks after intrastriatal 6-OHDA injections, coronal brain sections containing the SNpc were immunolabeled using anti-TH antibody. Scale bar = 200 μm. (C, D) Stereological counting of TH+ neurons in each (C) ipsilateral (IPSI) or (D) contralateral (CON) side of the SNpc using 6 slices per animal. Data are presented as mean ± standard error. N = 3-5 per group. Two-way analysis of variance was followed by Tukey's post-hoc test; #p < 0.05, ###p < 0.001 versus VEH-injected group; *p < 0.05 versus WT mice; †p < 0.05, ††p < 0.01, †††p < 0.001 among different time points.

using TH immunostaining after 6-OHDA injection (Figs. 2A and 2B). Both WT and RKO mice exhibited significantly less ipsilateral TH-positive SNpc neurons 3 days after 6-OHDA injection than their VEH-injected genotype-matched controls, but there was no significant difference between WT and RKO mice (Fig. 2C). RKO mice exhibited a greater decrease in the number of SNpc DAergic neurons compared to WT mice 1- and 2-weeks after 6-OHDA injection despite the similar number of TH-positive cells between VEH-injected WT and RKO mice throughout the experiment (Fig. 2C). Significant decreases in the number of TH-positive neurons in the ipsilateral SNpc were only apparent 3 days and 2 weeks post-6-OHDA injection in WT mice; however, this number decreased considerably 3 days, 1 week, and 2 weeks post-injection in RKO mice, demonstrating a more rapid time-dependent decline (Fig. 2C; $F_{(2,33)} = 15.940$, $p < 0.001$ for time, $F_{(3,33)} = 87.450$, $p < 0.001$ among groups, and $F_{(6,33)} = 7.297$, $p < 0.001$ for interaction). In contrast to the ipsilateral side, DAergic neurons in the contralateral SNpc were not affected by 6-OHDA lesion in any of the mice (Fig. 2D).

Intrastriatal injection of 6-OHDA causes progressive DAergic degeneration not only in the SNpc, but also in the VTA (Dauer and Przedborski, 2003; Sauer and Oertel, 1994). We therefore examined 6-OHDA-induced TH-positive DAergic neuronal loss in the VTA. Interestingly, differential genotype-specific patterns of TH-positive neuronal loss were observed in the VTA (Figs. 2A and 3A). Three days after 6-OHDA injection, there was no evidence of 6-OHDA-induced TH-positive DAergic neuronal loss in the ipsilateral VTA in both genotypes (Fig. 3B). However, TH-positive neuronal loss in the ipsilateral VTA was apparent beginning 1-week after 6-OHDA injection in both genotypes (Fig. 3B). The reduction in TH-positive cells was not significantly different between 1- and 2-weeks after 6-OHDA injection in the ipsilateral VTA of WT mice (Fig. 3B). However, TH-positive neurons in the ipsilateral VTA of RKO animals decreased in a time-dependent manner up to 2-weeks after 6-OHDA treatment (Fig. 3B; $F_{(2,33)} = 34.790$, $p < 0.001$ for time, $F_{(3,33)} = 48.150$, $p < 0.001$ among groups and $F_{(6,33)} = 18.110$, $p < 0.001$ for interaction). In contrast to the ipsilateral side, DAergic neurons in the contralateral VTA were not affected by the 6-OHDA lesion (Fig. 3C).

We also examined 6-OHDA-dependent TH expression pattern in VMB tissues including SNpc and VTA of WT and RKO mice by western blot analysis (Fig. 4). Although 6-OHDA significantly alleviated the TH expression in ipsilateral VMB from both WT and RKO compared to VEH-treated mice at 2

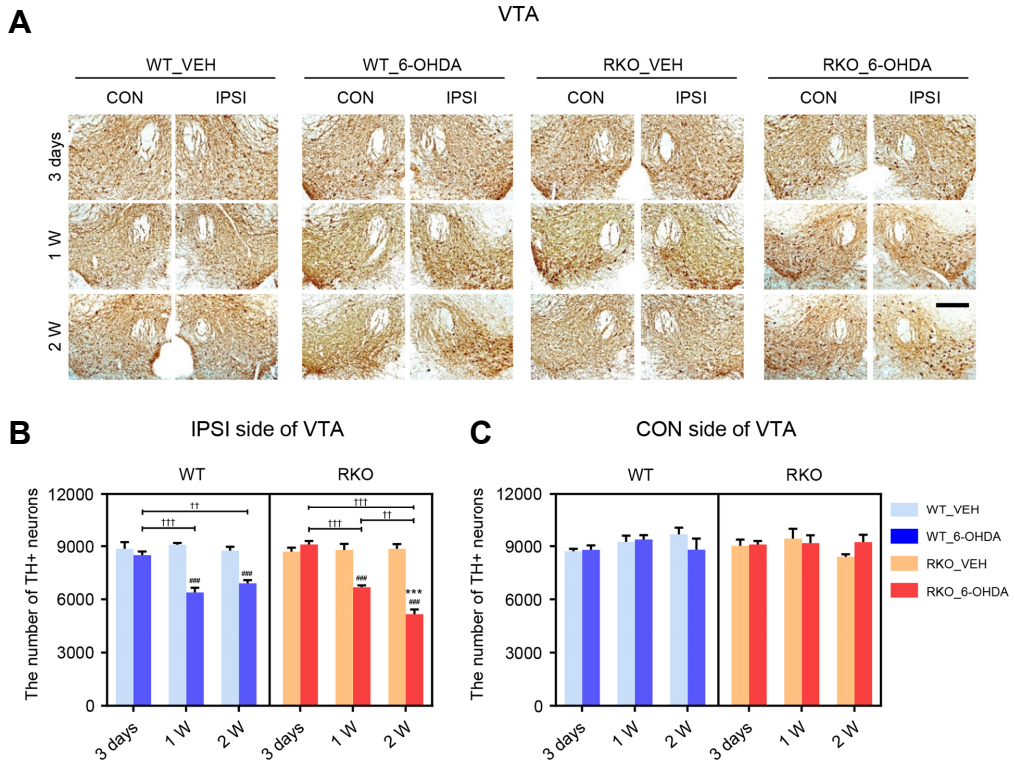

Fig. 3. 6-hydroxydoapmine (6-OHDA)-injected *Rev-erbα* knockout (RKO) mice exhibit greater, accelerated dopaminergic neuronal loss in the VTA. (A) Three days, 1 week, and 2 weeks after intrastriatal 6-OHDA injections, coronal brain sections containing the ventral tegmental area (VTA) were immunolabeled using tyrosine hydroxylase (TH) antibody. Scale bar = 200 μm. (B, C) Stereological counting of TH+ neurons in each (B) ipsilateral (IPSI) or (C) contralateral (CON) side of the VTA using 6 slices per animal. Data are presented as mean ± standard error. N = 3-4 per group. Two-way analysis of variance was followed by Tukey's post-hoc test; ###p < 0.001 versus VEH-injected group; ***p < 0.001 versus WT mice; ††p < 0.01, †††p < 0.001 among different time points.

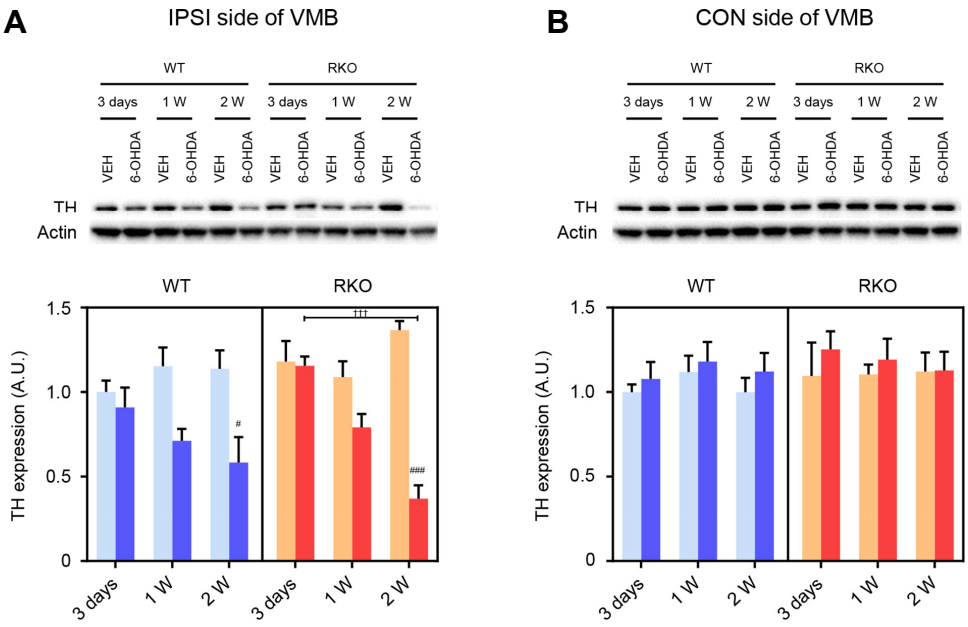

Fig. 4. *Rev-erbα* knockout (RKO) mice show a much sharper decline in tyrosine hydroxylase (TH) expression in the ventral midbrain (VMB) compared to WT mice following 6-hydroxydopamine (6-OHDA) injection. (A, B) Western blotting was performed in each (A) ipsilateral (IPSI) or contralateral (CON) side of the VMB with analysis of anti-TH and anti-β-actin antibodies. Representative blots were shown in upper panel. Relative TH immunoreactivities were presented as arbitrary units relative to WT mice 3 days after vehicle (VEH) injection. Data are presented as mean ± standard error. N = 4 per group in IPSI side. N = 3 per group in CON side. Two-way analysis of variance was followed by Tukey's post-hoc test; #p < 0.03, ###p < 0.001 versus VEH-injected group; +++p < 0.001 among different time points.

weeks following injection, RKO mice showed a much sharper decline in this protein levels compared to WT mice according to time passed after 6-OHDA treatment (Fig. 4A; $F_{(2,36)}$ = 4.246, $p < 0.05$ for time, $F_{(3,36)}$ = 18.020, $p < 0.001$ among groups, and $F_{(6,36)}$ = 6.040, $p < 0.001$ for interaction). However, TH expression in contralateral VMB was not affected either by genotype and neurotoxin (Fig. 4B).

Prolonged proliferation of microglial cells, but not astrocytes by 6-OHDA in RKO mice

The pathogenesis and progression of PD is often associated with neuroinflammatory processes, including cytokine overproduction and microglial activation. In the 6-OHDA-induced PD model, resident immune cells in the central nervous system reflect neuroinflammation (Haas et al., 2016; Marinova-Mutafchieva et al., 2009; Walsh et al., 2011). The SN sections from 6-OHDA-injected mice were stained with IBA1 to visualize microglial cell populations (Fig. 4A). Significant changes in the number of microglia were not observed in the ipsilateral SN 3-days after 6-OHDA injection in any of the mice (Fig. 4B). Notably, 6-OHDA injection led to a transient increase in the total number of IBA1-positive cells 1-week after injection in WT mice, whereas a prolonged increase was found in RKO mice (Fig. 4B; $F_{(2,33)}$ = 8.894, $p < 0.001$ for time, $F_{(3,33)}$ = 24.45, $p < 0.001$ among groups, and $F_{(6,33)}$ = 3.531, $p < 0.01$ for interaction). The number of IBA1-positive cells in VEH-treated animals was not significantly different between genotypes at any of the tested time points (Fig. 4B). The neurotoxin barely affected microglial cells in the contralateral side (Fig. 4C). We then examined the astrocytic response in the SN by immunostaining for GFAP, an astrocyte marker (Fig. 5A). There was a similar time-dependent increase in the proliferation of astrocytes in the ipsilateral SN in both genotypes (Fig. 5B; $F_{(2,36)}$ = 8.295, $p < 0.01$ for time, $F_{(3,36)}$ = 40.010, $p < 0.001$ among groups, and $F_{(6,36)}$ = 4.848, $p < 0.01$ for interaction). The number of GFAP-positive cells in VEH-treated animals was not significantly different between genotypes at any of the time tested points, and the neurotoxin barely affected contralateral astrocytes (Figs. 5B and 5C). Therefore, REV-ERBα deficiency may evoke prolonged proliferation of microglia, but not astrocytes, at the sites damaged by 6-OHDA.

Alterations in inflammation-related cytokines in RKO mice

Various pro-inflammatory cytokines are involved in neuroinflammation (Hirsch and Hunot, 2009; Tansey and Goldberg, 2010). We obtained VMB tissue from mice sacrificed 1 week after 6-OHDA injection and examined whether there were altered mRNA expression profiles for pro-inflammatory cytokines in RKO mice. The present study tested 3 cytokines, *IL-1β*, *TNFα*, and *IL-6*. Compared to 6-OHDA-injected WT and VEH-injected mutant mice, 6-OHDA-injected RKO mice exhibited significantly higher levels of *IL-1β* mRNA in the ipsilateral VMB (Fig. 6A; $F_{(1,40)}$ = 6.273, $p < 0.05$ for genotype, $F_{(3,40)}$ = 7.965, $p < 0.001$ for treatment, and $F_{(3,40)}$ = 2.280, p = 0.094 for interaction). *TNFα* mRNA expression was affected by 6-OHDA treatment, but this was not significantly different between genotypes (Fig. 6B; $F_{(1,42)}$ = 1.910, p = 0.174

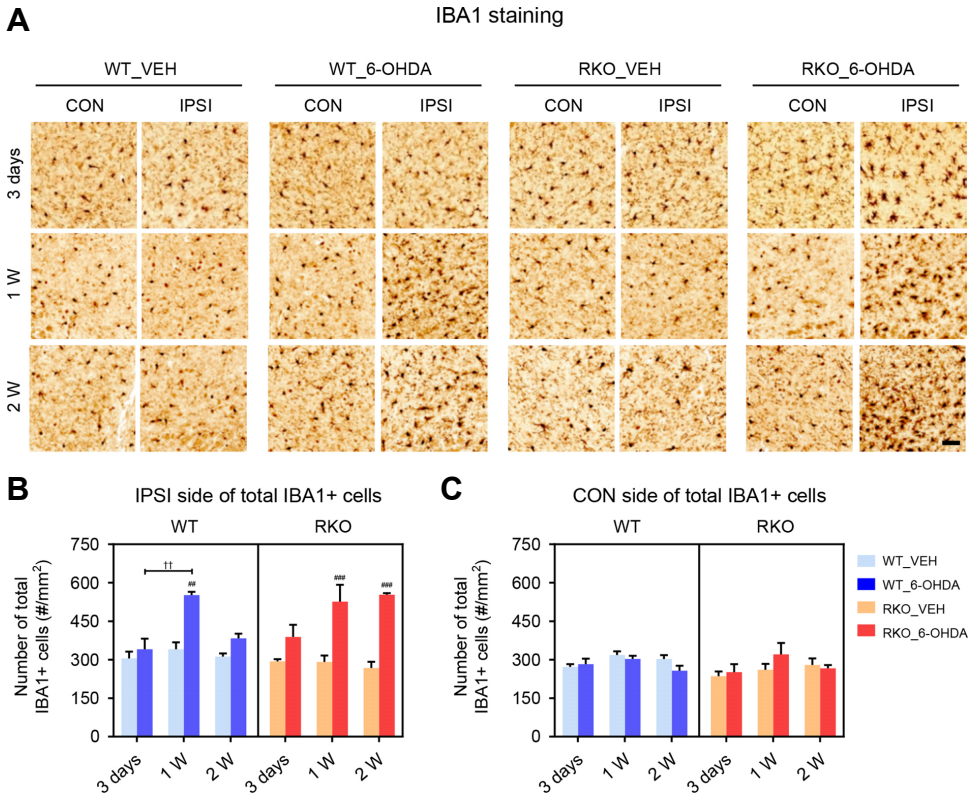

Fig. 5. REV-ERBα deficiency prolongs 6-hydroxydoapmine (6-OHDA)-induced proliferation of the microglia in the substantia nigra (SN). (A) Representative images immunostained for ionized calcium-binding adapter molecule 1 (IBA1) in the SN 3 days, 1 week, and 2 weeks after injection. Scale bar = 50 μm. (B, C) The numbers of total IBA1-positive microglia per mm^2 in each (B) ipsilateral (IPSI) and (C) contralateral (CON) side of the SN. Data are presented as mean ± standard error. N = 3-4 per group. Two-way analysis of variance was followed by Tukey's post-hoc test; ##p < 0.01, ###p < 0.001 versus VEH-injected group; ††p < 0.01 among different time points.

for genotype, $F_{(3,42)}$ = 5.095, p < 0.01 for treatment, and $F_{(3,42)}$ = 0.306, p = 0.821 for interaction). Although *IL-6* mRNA expression was significantly different between WT and RKO mice, it was not significantly affected by 6-OHDA administration (Fig. 6C; $F_{(1,43)}$ = 6.826, p < 0.05 for genotype, $F_{(3,43)}$ =0.685, p = 0.566 for treatment, and $F_{(3,43)}$ = 0.640, p = 0.594 for interaction). We then examined the protein contents of IL-1β in the VMB lysates at different time points after VEH or 6-OHDA injections. Midbrain IL-1β content was not significantly affected by genotype or 6-OHDA treatment 3 days after injection (Fig. 6D, left panel; $F_{(1,24)}$ = 0.325, p = 0.574 for genotype, $F_{(3,24)}$ = 0.133, p = 0.939 for treatment, and $F_{(3,24)}$ = 0.524, p = 0.670 for interaction). Consistent with its mRNA expression profiles, IL-1β content in ipsilateral VMB tissue was significantly increased 1 week after 6-OHDA injection (Fig. 6D, middle panel; $F_{(1,24)}$ = 6.635, p < 0.05 for genotype, $F_{(3,24)}$ = 8.122, p < 0.001 for treatment, and $F_{(3,24)}$ = 4.394, p < 0.05 for interaction). Induced IL-1β protein levels in 6-OHDA-injected RKO mice were reduced, but still higher than in 6-OHDA-injected WT mice 2-weeks after treatment (Fig. 6D, right panel; $F_{(1,32)}$ = 12.090, p < 0.01 for genotype, $F_{(3,32)}$ = 9.777, p < 0.001 for treatment, and $F_{(3,32)}$ = 3.541, p < 0.05 for interaction). These findings suggest that 6-OHDA-induced IL-1β production is potentiated in RKO mice, presumably by a mechanism involving IL-1β gene expression, which may in turn contribute to exacerbation of 6-OHDA-induced PD symptoms in these mice.

DISCUSSION

The present study demonstrates that REV-ERBα deficiency accelerates and exacerbates DA-related motor symptoms in a mouse model of PD. RKO mice exhibited more severe locomotor asymmetry and motor coordination impairment relative to WT controls. Consistent with such motor defects, REV-ERBα deficiency was associated with increased 6-OHDA-induced DAergic degeneration in both the SNpc and VTA in addition to prolonged microglial proliferation. Accompanying mRNA and protein findings suggest that enhanced neuroinflammation by robust IL-1β production may be involved in the augmented pathological phenotypes in RKO mice.

It is widely accepted that sleep and circadian problems in PD patients are key non-motor symptoms of the neurodegenerative disease. More importantly, recent studies imply that circadian disruption by either environmental or genetic causes may serve as a significant risk factor for PD (Abbott et al., 2005; Comella, 2006; Gu et al., 2015; Lauretti et al., 2017).

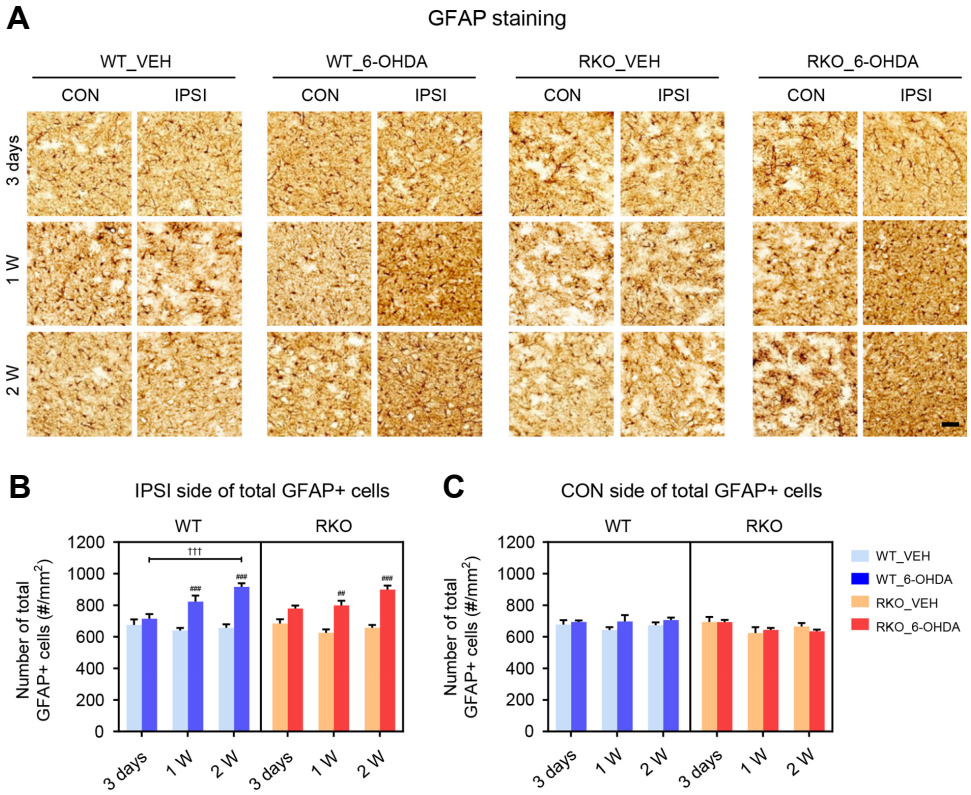

Fig. 6. REV-ERBα deficiency does not affect astrogliosis induced by 6-OHDA in the substantia nigra (SN). (A) Representative immunohistochemistry findings for glial fibrillary acidic protein (GFAP) in the SN 3 days, 1 week, and 2 weeks after injection. Scale bar = 50 μm. (B, C) The number of total GFAP-positive astrocytes per mm^2 in each (B) ipsilateral (IPSI) and (C) contralateral (CON) side of the SN. Two-way analysis of variance was followed by Tukey's post-hoc test; ##p < 0.01, ###p < 0.001 versus VEH-injected group; †††p < 0.001 versus among different time points.

Notably, PD patients have blunted rhythm of *BMAL1* expression in peripheral blood cells, with sleep disturbances (Breen et al., 2014). Alterations in circadian behaviors and clock gene expression in the suprachiasmatic nucleus (SCN) were recently reported in various animal models of PD (Fifel et al., 2014; Hayashi et al., 2013; Kudo et al., 2011). Genetic abrogation of BMAL1, an uppermost regulator of the circadian clock, induced age-dependent astrogliosis, oxidative stress through the dysregulation of redox defense genes, and enhanced neurodegeneration in the presence of neurotoxic insults (Musiek et al., 2013). However, how the internal misalignment of the circadian system is and which members of the circadian molecular clock are associated with the onset and progression of PD, still remain to be elucidated. In this regard, it is noteworthy that impaired REV-ERBα function leads to instability of the intrinsic rhythms as a key component of the stabilizing loop (Preitner et al., 2002) as well as dysregulation of sleep homeostasis and architecture (Mang et al., 2016). Such dysfunctional circadian rhythmicity in RKO mice may have contributed to the increased susceptibility to the neurotoxin observed in 6-OHDA-induced DA neuronal loss.

We found a temporal relationship between DAergic neurodegeneration and neuroinflammation in the 6-OHDA-induced PD model in WT and RKO mice. DAergic neuronal loss in the SN was apparent 3 days after 6-OHDA lesion in both genotypes and progressively worsened thereafter, consistent with previous reports that 25-35% of DAergic neurons were lost within 3-4 days post-intrastriatal 6-OHDA lesion in mice (Alvarez-Fischer et al., 2008; Virgone-Carlotta et al., 2013). Although RKO mice exhibited DAergic neuronal loss in the SN 3 days after 6-OHDA injection similar to WT mice, the mutant mice exhibited a more rapid and progressive DAergic degeneration in both the SN and VTA, implying that REV-ERBα is involved in the progression of PD-like symptoms. We found that microglial density transiently increased 1-week post-injection, returning to basal level in the SN 2 weeks following 6-OHDA-injection in WT mice. The results are comparable to previous studies (Akiyama and McGeer, 1989; Marinova-Mutafchieva et al., 2009). Considering that maximum proliferation of microglia 1-week post-6-OHDA lesion in WT mice is accompanied by a significant decrease in the number of DA neuronal cell bodies in the SN, microglia activation may precede DAergic neuronal loss at later time points. In this regard, our observation that RKO mice exerted sustained microglial proliferation and hyperactivation along with more severe DAergic neuronal loss in response to 6-OHDA is important. Taken together, prolonged

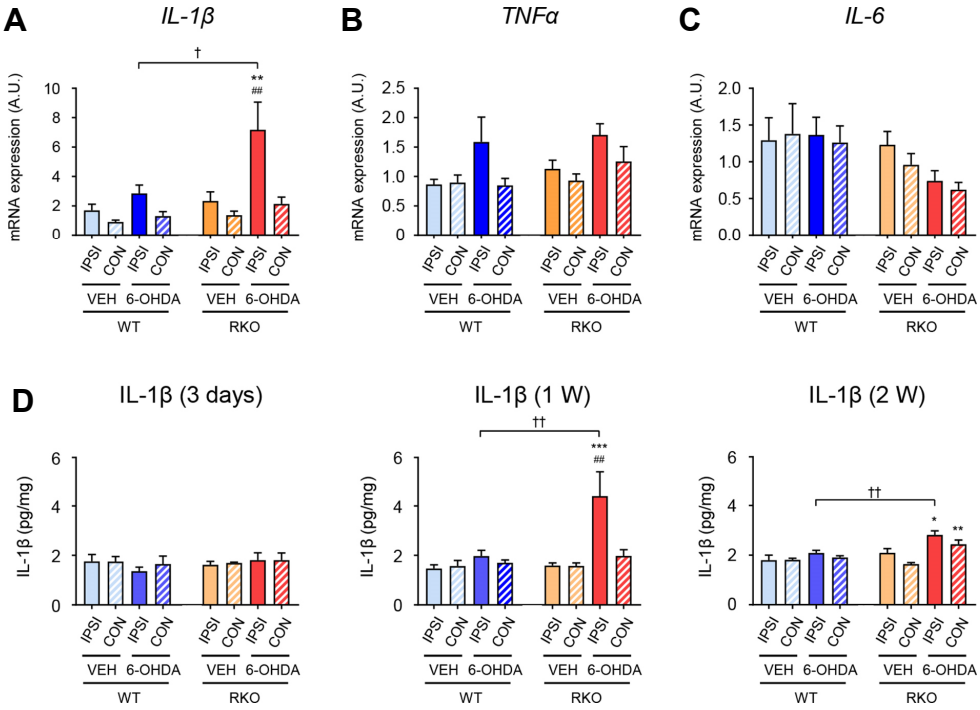

Fig. 7. Expression of gliosis-related cytokines are altered in the ventral midbrain (VMB) tissue of *Rev-erbα* knockout (RKO) mice after 6-hydroxydoapmine (6-OHDA) injection. mRNA expression of pro-inflammatory cytokines in the ipsilateral (IPSI) and contralateral (CON) side of the VMB 1 week after injection. (A) *IL-1β*: interleukin 1 beta, (B) *TNFα*: tumor necrosis factor alpha, and (C) *IL-6*: interleukin 6. Data are presented as mean ± standard error. N = 5-7 per group. Two-way analysis of variance was followed by Tukey's post-hoc test; ##p < 0.01 versus contralateral side; **p < 0.01 versus VEH-treated group; †p < 0.05 versus WT mice. (D) Enzyme-linked immunosorbent assay (ELISA) of protein levels of interleukin-1β (IL-1β). The protein levels of IL-1β in the IPSI and CON side of the VMB 3 days, 1 week, and 2 weeks after injection. Data are presented as mean ± standard error. N = 3-6 per group. Two-way analysis of variance was followed by Tukey's post-hoc test; ##p < 0.01 versus contralateral side; *p < 0.05, **p < 0.01, ***p < 0.001 versus VEH-treated group; ††p < 0.01 versus WT mice.

microglial activation may exacerbate DAergic neurodegeneration in RKO mice exposed to 6-OHDA.

Neuroinflammation is known to be heavily involved in the progression of PD through its impacts on both DAergic neuronal death and microglial proliferation (Hirsch and Hunot, 2009; Tansey and Goldberg, 2010). The prolonged microglial activation in RKO mice strongly suggests a potentiation of neuroinflammatory responses to 6-OHDA. Over-production of the pro-inflammatory cytokine IL-1β in RKO mice is thus noteworthy. Indeed, microglial proliferation in the SN and increased production of pro-inflammatory cytokines in postmortem striatal tissue have been observed in PD patients (McGeer et al., 1988; Mogi et al., 1994a; 1994b). Furthermore, several pro-inflammatory cytokines are augmented even in the cerebrospinal fluid of PD patients (Blum-Degena et al., 1995; Mogi et al., 1994b). Among such PD-related cytokines, IL-1β appears to have a causal role in neuroinflammation-mediated PD pathology. Chronic expression of IL-1β in the SN is sufficient to result in progressive DAergic neuronal death and motor deficits as well as activation of both microglia and astrocytes (Ferrari et al., 2006), suggesting sustained expression of IL-1β in the RKO may be responsible for the exacerbation of neuroinflammation-associated neuronal damage.

Circadian clock proteins have been implicated in the rhythmic properties found in immune and inflammation systems. Immune parameters change with the time of day and circadian rhythm disruptions have been linked to inflammatory pathologies (Gibbs et al., 2012). In this regard, it is noteworthy that both basal and immune challenge-induced production of pro-inflammatory cytokines follow circadian oscillations, suggesting that the production of cytokines as well as their signaling molecules may be under the control of circadian clocks (Fonken et al., 2015; Keller et al., 2009). In accordance, expression of pro-inflammatory cytokines, including IL-1β, along with microglia inflammatory responses are thought to be linked to an intrinsic circadian clock (Fonken et al., 2015). It is important that some cytokines, such as IL-1β, are negatively controlled by the circadian molecular clock in a cell-autonomous manner. For example, cell-type specific deletion of the gene *Bmal1* in monocytes results in enhanced production of IL-1β and IL-6 (Nguyen et al., 2013). Considering its transcriptional repressive activity on a wide range of target genes (Chung et al., 2014; Preitner et al., 2002), REV-ERBα may mediate the suppressive actions of BMAL1 on IL-1β production. These findings

collectively suggest that the cellular circadian clock may gate immune and inflammatory responses, and often limit hyperactivation of these responses. It is therefore plausible that 6-OHDA-induced neuroinflammatory responses are not properly terminated in the absence of functional REV-ERBα and the accompanying uncontrolled responses contribute to the exacerbation of DAergic degeneration.

In conclusion, our study shows that REV-ERBα has a significant role in protecting DAergic neurons from 6-OHDA-induced degeneration, presumably by inhibiting overactivation of neuroinflammatory responses. Considering that circadian dysfunction is a common symptomatic hallmark of various devastating neurodegenerative conditions, such as PD, Alzheimer's disease, and Huntington's disease (Videnovic et al., 2014), the present study can be extended to understand the interplay between the circadian system and various neurodegenerative diseases. Furthermore, it should be noted that REV-ERBα is one of the most highlighted targets for pharmacological modulation of the mammalian circadian molecular clock. A potent synthetic agonist and antagonist have already been developed and their effectiveness in altering circadian gene expression and producing diverse physiological outputs has been proven (Banerjee et al., 2014; Kojetin et al., 2010; Solt et al., 2012). Further understanding of the link between REV-ERBα and PD may result in novel therapeutic approaches to PD as well as valuable insights into its pathogenesis.

ACKNOWLEDGMENTS

We thank Dr. U. Schibler (University of Geneva) for providing *Rev-erbα* mutant mice. This work was supported by the Ministry of Science, ICT and Future Planning through the National Research Foundation of Korea (NRF-2017R1A2A1A05001351 to K. Kim and NRF-2016M3C7A1904340 to G. H. Son). K. Kim was supported by DGIST Start-up Fund Program (2018010086).

REFERENCES

Abbott, R., Ross, G., White, L., Tanner, C., Masaki, K., Nelson, J., Curb, J., and Petrovitch, H. (2005). Excessive daytime sleepiness and subsequent development of Parkinson disease. Neurology *65*, 1442-1446.

Akiyama, H., and McGeer, P.L. (1989). Microglial response to 6-hydroxydopamine-induced substantia nigra lesions. Brain Res. *489*, 247-253.

Alvarez-Fischer, D., Henze, C., Strenzke, C., Westrich, J., Ferger, B., Höglinger, G.U., Oertel, W.H., and Hartmann, A. (2008). Characterization of the striatal 6-OHDA model of Parkinson's disease in wild type and α-synuclein-deleted mice. Exp. Neurol. *210*, 182-193.

Banerjee, S., Wang, Y., Solt, L.A., Griffett, K., Kazantzis, M., Amador, A., El-Gendy, B.M., Huitron-Resendiz, S., Roberts, A.J., Shin, Y., et al. (2014). Pharmacological targeting of the mammalian clock regulates sleep architecture and emotional behaviour. Nat. Commun. *5*, 5759.

Bechtold, D.A., Gibbs, J.E., and Loudon, A.S. (2010). Circadian dysfunction in disease. Trends. Pharmacol. Sci. *31*, 191-198.

Blum-Degena, D., Müller, T., Kuhn, W., Gerlach, M., Przuntek, H., and Riederer, P. (1995). Interleukin-1β and interleukin-6 are elevated in the cerebrospinal fluid of Alzheimer's and de novo Parkinson's disease patients. Neurosci. Lett. *202*, 17-20.

Breen, D.P., Vuono, R., Nawarathna, U., Fisher, K., Shneerson, J.M., Reddy, A.B., and Barker, R.A. (2014). Sleep and circadian rhythm regulation in early Parkinson disease. JAMA Neurol. *71*, 589-595.

Chung, S., Lee, E.J., Yun, S., Choe, H.K., Park, S.B., Son, H.J., Kim, K.S., Dluzen, D.E., Lee, I., Hwang, O., et al. (2014). Impact of circadian nuclear receptor REV-ERBalpha on midbrain dopamine production and mood regulation. Cell *157*, 858-868.

Comella, C.L. (2006). Sleep disturbances and excessive daytime sleepiness in Parkinson disease: an overview. J. Neural Transm. Suppl. *70*, 349-355.

Dauer, W., and Przedborski, S. (2003). Parkinson's disease: mechanisms and models. Neuron *39*, 889-909.

Everett, L.J., and Lazar, M.A. (2014). Nuclear receptor Rev-erbα: up, down, and all around. Trends. Endocrinol. Metab. *25*, 586-592.

Ferrari, C.C., Godoy, M.C.P., Tarelli, R., Chertoff, M., Depino, A.M., and Pitossi, F.J. (2006). Progressive neurodegeneration and motor disabilities induced by chronic expression of IL-1β in the substantia nigra. Neurobiol. Dis. 24, 183-193.

Fifel, K., Vezoli, J., Dzahini, K., Claustrat, B., Leviel, V., Kennedy, H., Procyk, E., Dkhissi-Benyahya, O., Gronfier, C., and Cooper, H.M. (2014). Alteration of daily and circadian rhythms following dopamine depletion in MPTP treated non-human primates. PLoS One *9*, e86240.

Fonken, L.K., Frank, M.G., Kitt, M.M., Barrientos, R.M., Watkins, L.R., and Maier, S.F. (2015). Microglia inflammatory responses are controlled by an intrinsic circadian clock. Brain Behav. Immun. *45*, 171-179.

Gibbs, J.E., Blaikley, J., Beesley, S., Matthews, L., Simpson, K.D., Boyce, S.H., Farrow, S.N., Else, K.J., Singh, D., Ray, D.W., et al. (2012). The nuclear receptor REV-ERBα mediates circadian regulation of innate immunity through selective regulation of inflammatory cytokines. Proc. Natl. Acad. Sci. USA *109*, 582-587.

Gu, Z., Wang, B., Zhang, Y.B., Ding, H., Zhang, Y., Yu, J., Gu, M., Chan, P., and Cai, Y. (2015). Association of ARNTL and PER1 genes with Parkinson's disease: a case-control study of Han Chinese. Sci. Rep. *5*, 15891.

Guillaumond, F., Dardente, H., Giguere, V., and Cermakian, N. (2005). Differential control of Bmal1 circadian transcription by REV-ERB and ROR nuclear receptors. J. Biol. Rhythms *20*, 391-403.

Haas, S.J., Zhou, X., Machado, V., Wree, A., Krieglstein, K., and Spittau, B. (2016). Expression of Tgfbeta1 and Inflammatory Markers in the 6-hydroxydopamine Mouse Model of Parkinson's Disease. Front. Mol. Neurosci. *9*, 7.

Hayashi, A., Matsunaga, N., Okazaki, H., Kakimoto, K., Kimura, Y., Azuma, H., Ikeda, E., Shiba, T., Yamato, M., Yamada, K.i., et al. (2013). A disruption mechanism of the molecular clock in a MPTP mouse model of Parkinson's disease. Neuromol. Med. *15*, 238-251.

Hirsch, E.C., and Hunot, S. (2009). Neuroinflammation in Parkinson's disease: a target for neuroprotection? Lancet Neurol. *8*, 382-397.

Keller, M., Mazuch, J., Abraham, U., Eom, G.D., Herzog, E.D., Volk, H.D., Kramer, A., and Maier, B. (2009). A circadian clock in macrophages controls inflammatory immune responses. Proc. Natl. Acad. Sci. USA *106*, 21407-21412.

Kim, T.W., Moon, Y., Kim, K., Lee, J.E., Koh, H.C., Kim, H., and Sun, W. (2011). Dissociation of progressive dopaminergic neuronal death and behavioral impairments by Bax deletion in a mouse model of Parkinson's diseases. PloS One *6*, e25346.

Kojetin, D., Wang, Y., Kamenecka, T.M., and Burris, T.P. (2010). Identification of SR8278, a synthetic antagonist of the nuclear heme receptor REV-ERB. ACS Chem. Biol. *6*, 131-134.

Kondratova, A.A., and Kondratov, R.V. (2012). Circadian clock and

pathology of the ageing brain. Nat. Rev. Neurosci. *13*, 325.

Kudo, T., Loh, D.H., Truong, D., Wu, Y., and Colwell, C.S. (2011). Circadian dysfunction in a mouse model of Parkinson's disease. Exp. Neurol. *232*, 66-75.

Lauretti, E., Di Meco, A., Merali, S., and Pratico, D. (2017). Circadian rhythm dysfunction: a novel environmental risk factor for Parkinson's disease. Mol. Psychiatry *22*, 280-286.

Mang, G.M., La Spada, F., Emmenegger, Y., Chappuis, S., Ripperger, J.A., Albrecht, U., and Franken, P. (2016). Altered Sleep Homeostasis in Rev-erb α Knockout Mice. Sleep *39*, 589-601.

Marinova-Mutafchieva, L., Sadeghian, M., Broom, L., Davis, J.B., Medhurst, A.D., and Dexter, D.T. (2009). Relationship between microglial activation and dopaminergic neuronal loss in the substantia nigra: a time course study in a 6-hydroxydopamine model of Parkinson's disease. J. Neurochem. *110*, 966-975.

McGeer, P., Itagaki, S., Boyes, B., and McGeer, E. (1988). Reactive microglia are positive for HLA-DR in the substantia nigra of Parkinson's and Alzheimer's disease brains. Neurology *38*, 1285-1285.

Mogi, M., Harada, M., Kondo, T., Riederer, P., Inagaki, H., Minami, M., and Nagatsu, T. (1994a). Interleukin-1β, interleukin-6, epidermal growth factor and transforming growth factor-α are elevated in the brain from parkinsonian patients. Neurosci. Lett. *180*, 147-150.

Mogi, M., Harada, M., Riederer, P., Narabayashi, H., Fujita, K., and Nagatsu, T. (1994b). Tumor necrosis factor-α (TNF-α) increases both in the brain and in the cerebrospinal fluid from parkinsonian patients. Neurosci. Lett. *165*, 208-210.

Monville, C., Torres, E.M., and Dunnett, S.B. (2006). Comparison of incremental and accelerating protocols of the rotarod test for the assessment of motor deficits in the 6-OHDA model. J. Neurosci. Methods *158*, 219-223.

Musiek, E.S., Lim, M.M., Yang, G., Bauer, A.Q., Qi, L., Lee, Y., Roh, J.H., Ortiz-Gonzalez, X., Dearborn, J.T., Culver, J.P., et al. (2013). Circadian clock proteins regulate neuronal redox homeostasis and neurodegeneration. J. Clin. Invest. *123*, 5389-5400.

Nguyen, K.D., Fentress, S.J., Qiu, Y., Yun, K., Cox, J.S., and Chawla, A. (2013). Circadian gene Bmal1 regulates diurnal oscillations of Ly6C(hi) inflammatory monocytes. Science *341*, 1483-1488.

Preitner, N., Damiola, F., Zakany, J., Duboule, D., Albrecht, U., and Schibler, U. (2002). The orphan nuclear receptor REV-ERBα controls circadian transcription within the positive limb of the mammalian circadian oscillator. Cell *110*, 251-260.

Sauer, H., and Oertel, W. (1994). Progressive degeneration of nigrostriatal dopamine neurons following intrastriatal terminal lesions with 6-hydroxydopamine: a combined retrograde tracing and immunocytochemical study in the rat. Neuroscience *59*, 401-415.

Solt, L.A., Wang, Y., Banerjee, S., Hughes, T., Kojetin, D.J., Lundasen, T., Shin, Y., Liu, J., Cameron, M.D., Noel, R., et al. (2012). Regulation of circadian behavior and metabolism by synthetic REV-ERB agonists. Nature *485*, 62-68.

Tansey, M.G., and Goldberg, M.S. (2010). Neuroinflammation in Parkinson's disease: its role in neuronal death and implications for therapeutic intervention. Neurobiol. Dis. *37*, 510-518.

Videnovic, A., Lazar, A.S., Barker, R.A., and Overeem, S. (2014). 'The clocks that time us'—circadian rhythms in neurodegenerative disorders. Nat. Rev. Neurol. *10*, 683-693.

Virgone-Carlotta, A., Uhlrich, J., Akram, M.N., Ressnikoff, D., Chrétien, F., Domenget, C., Gherardi, R., Despars, G., Jurdic, P., Honnorat, J., et al. (2013). Mapping and kinetics of microglia/neuron cell-to-cell contacts in the 6-OHDA murine model of Parkinson's disease. Glia *61*, 1645-1658.

Walsh, S., Finn, D., and Dowd, E. (2011). Time-course of nigrostriatal neurodegeneration and neuroinflammation in the 6-hydroxydopamine-induced axonal and terminal lesion models of Parkinson's disease in the rat. Neuroscience *175*, 251-261.

Warner, T.T., and Schapira, A.H. (2003). Genetic and environmental factors in the cause of Parkinson's disease. Ann. Neurol. *53 Suppl 3*, S16-23.

Woldt, E., Sebti, Y., Solt, L.A., Duhem, C., Lancel, S., Eeckhoute, J., Hesselink, M.K., Paquet, C., Delhaye, S., Shin, Y., et al. (2013). Rev-erb-α modulates skeletal muscle oxidative capacity by regulating mitochondrial biogenesis and autophagy. Nat. Med. *19*, 1039-1046.